Performance Evaluation and Simulation of a Solar Thermal Power Plant

Eduardo I. Ortiz-Rivera
Member, IEEE
University of Puerto Rico
Post Street
Mayaguez, PR 00680, USA
eduardo.ortiz@ece.uprm.edu

Luisa I. Feliciano-Cruz
Student Member, IEEE
University of Puerto Rico
Post Street
Mayaguez, PR 00680, USA
luisa.izette@gmail.com

***Abstract* -- This paper presents a Simulink® Model that has been developed for the performance evaluation and simulation of Solar Power Generating or Solar Thermal Power Plants in Puerto Rico with the Compound Parabolic Concentrator as the solar collector of choice. There are several costly and sophisticated commercial software programs that perform this task but, this tool is aimed at performing initial evaluations of the viability and technical feasibility of these types of systems in terms of outlet temperature from the collector field and power output produced. It takes into consideration local solar radiation data and atmospheric conditions, as well as collector data and other parameters that can be adjusted by the user.**

***Index Terms*-- Solar energy, Solar power generation, Simulation, Modeling.**

I. INTRODUCTION

The increasing instability of fossil fuel costs has led the world in a quest for exploiting the free and naturally available energy from the Sun to produce electric power and, Puerto Rico is no exception. A performance evaluation and simulation of a Solar Thermal Power Plant is conducted for Puerto Rico, with local solar data, for determining the viability of the proposed project. As can be found in literature [1]-[6], several of the simulation studies that have been performed rely on parabolic troughs, costly software packages and on prototype system measurements usually conducted where solar radiation is the highest in the world. This model will show how system behavior is affected during solar transients in tropical regions taking into account solar variability throughout the day.

The use of the compound parabolic concentrator proves useful due to its non-imaging characteristics. This allows the solar collection system to concentrate direct, as well as diffuse radiation energy, as opposed to the parabolic trough which can only concentrate direct solar energy [7]. Since PR lies on a tropical region, solar energy is highly scattered mainly due to atmospheric phenomena such as: clouds, water vapor and dust particles [8]. The fact that the concentrator can accept diffuse solar energy greatly enhances its overall efficiency.

For the present study, an optical and thermal analysis of the CPC and absorber was conducted in Microsoft® Excel® and MATLAB®. The results were used in the Simulink® model constructed. These parameters can, however, be: estimated, taken from literature or from manufacturer's data. The HTF used in the analysis is molten salt. It is being preferred over the typical HTF, VP-1®, because it provides several advantages like: thermal energy storage (TES) medium, and chemical stability can attain higher operating temperatures [9]. Table 1 presents the data used in the analysis.

II. SOLAR RESOURCE AND STPP OVERVIEW

A. The Solar Resource

To better understand the solar resource as a means of harvesting it for energy production, several of the Sun's characteristics must be studied. Acknowledging these characteristics provide a basis for understanding, using and predicting solar radiation data [8]. It is important to recognize that there are two common methods which characterize solar radiation: the solar radiance or radiation, and solar insolation. Solar radiation is an instantaneous power density in units of kW/m^2 and solar insolation is the total amount of solar energy received at a particular location during a specified time period, in kWh/m^2 day or MJ/m^2 day.

On Earth's surface, radiation can be categorized as being beam, diffuse or global. Beam or direct radiation refers to the radiation received from the Sun without having been scattered by the atmosphere. Diffuse radiation is the one whose direction has been changed by scattering in the atmosphere due to clouds, water vapor, trees, etc. Global or total radiation is the sum of these two. It is important to acknowledge the type of solar radiation that a particular solar thermal system can effectively collect and the solar data available. Parabolic troughs, for example, can only utilize beam radiation obtained trough continuous tracking of the sun, whilst compound parabolic troughs can collect both beam and diffuse radiation without the need of continuous tracking.

B. How a Solar Thermal Power Plant Works?

Solar Thermal Power Plant (STPP) behaves like a conventional thermal power plant, but uses solar energy instead of a fossil fuel as a heat source for producing steam. Even though it is free, solar energy has two noteworthy disadvantages: energy density and availability [10]. There are several different ways in which a STPP can be designed, constructed and operated. It is usually the system components that dictate such designs. Fig. 1 shows a parabolic STPP schematic.

There can be variations, but the typical STPP (with a linear

geometry) contains the following components: collector array & solar tracking system (if needed), absorber, some sort of HTF (heat transfer fluid), heat transfer mechanisms such as: heat exchangers, condensers, etc, electromechanical devices such as: heat engines or generators for converting the HTF energy to electrical energy and if desired, some type of energy storage system and/or hybridization of the STPP for attending solar transients [11], [12].

III. STPP Analysis

A. The Compound Parabolic Concentrator (CPC)

The Compound Parabolic Concentrator (CPC) was conceived by Prof. Roland Winston in 1966 and is based on his research in the field of non-imaging optics. It makes use of the fact that when a parabola is tilted at an angle not equal to the direction of the beam radiation, the rays no longer concentrate on its focus; they are reflected instead in an area above and below the focus as can be seen in Fig. 2 [13]-[15].

If the half parabola that reflects above the focus is discarded and replaced with a similarly shaped parabola reflecting below the focus, the result is: a CPC, a concentrator that reflects (traps or funnels) all incoming rays from any angle between the focal line of the two parabola segments. The basic shape of the CPC is illustrated in Fig. 3. The angle that the axes of the parabola A and B make with axis of the CPC defines the acceptance angle θ, of the CPC. The acceptance half-angle, $\theta_{1/2}$, is the acceptance angle divided by two.

B. Optical Characteristics and Performance Analysis of CPC Collectors

Since the density of solar radiation incident on the Earth's surface is rather low, the only means to harvest it for electricity generation is through concentration. The concentration ratio **(***CR***)** of a collector can be stated as ratio of the input aperture area A_{aper} to the exit aperture area $A_{receiver}$, which based on the 2nd Law of Thermodynamics results in:

$$CR = \frac{A_{aper}}{A_{receiver}} = \frac{n_{ref}}{\sin\theta_{1/2}} \tag{1}$$

where n_{ref} is the index of refraction that can be approximated to 1 for air as a medium [13].

The optical performance of a CPC depends on whether the incident solar radiation is within the acceptance half-angle as stated before. A CPC's optical efficiency can be found by calculating the average number of reflections, $\langle n \rangle_i$ that radiation undergoes between the input aperture and the absorber or exit aperture, whichever is the case. The average number of reflections can be obtained by studying how the radiation that arrives at the collector travels between the absorber, reflector walls and if outside the acceptance angle, the radiation that comes back out of the CPC without being absorbed. By algebraically manipulating the relationships that lead to the average number of reflections, it can be shown that it only depends on the CPC's acceptance angle divided by two (or acceptance half angle) [13]:

$$\langle n \rangle_i = \frac{1}{2}(1+\sin\theta_{1/2})\times \left(\frac{\cos\theta_{1/2}}{\sin^2\theta_{1/2}} + \ln\frac{(1+\sin\theta_{1/2})(1+\cos\theta_{1/2})}{\sin\theta_{1/2}\left(\cos\theta_{1/2}+\sqrt{2(1+\sin\theta_{1/2})}\right)} - \frac{\sqrt{2}\cos\theta_{1/2}}{(1+\sin\theta_{1/2})^{3/2}} \right) - \frac{(1-\sin\theta_{1/2})(1+2\sin\theta_{1/2})}{2\sin^2\theta_{1/2}} \tag{2}$$

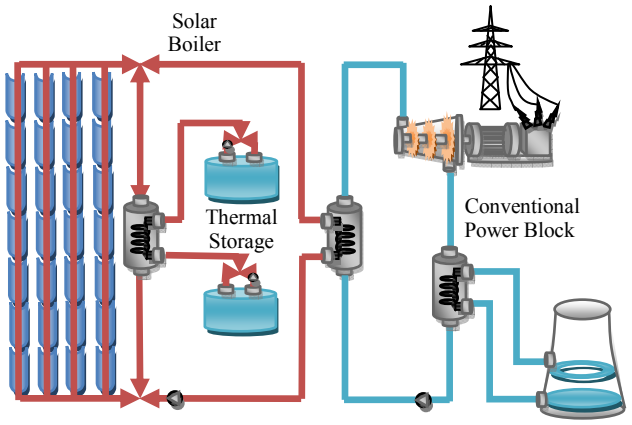

Fig. 1. Parabolic Solar Thermal Power Plant Schematic

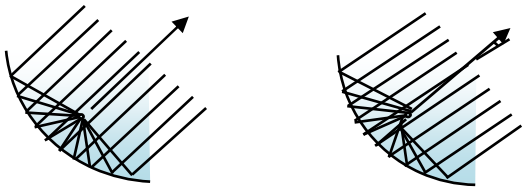

Fig. 2. Parabola intercepting solar radiation parallel to its axis (left) and not parallel to its axis (right). Adapted from [10].

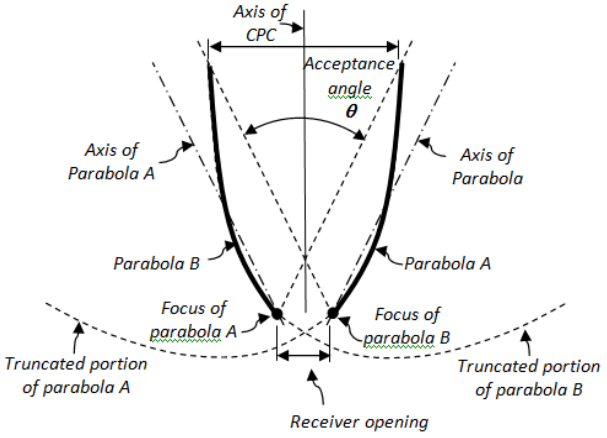

Fig. 3. Basic shape of a CPC. Adapted from [13].

After having studied all the pertinent factors regarding the optical performance of a CPC collector, its absorbed radiation per unit area of collector aperture S, can be estimated as [8]:

$$S = \rho_{CPC}^{\langle n \rangle_i} \alpha_r \tau_r \left(I_{b,CPC} + I_{d,CPC} \right) CR \tag{3}$$

$$I_{b,CPC} = F I_b \cos\theta_{1/2}$$

$$I_{d,CPC} = \begin{cases} \dfrac{I_d}{CR} & \text{for } (\beta + \theta_{1/2}) < 90^\circ \\ \dfrac{I_d}{2}\left(\dfrac{1}{CR} + \cos\beta \right) & \text{for } (\beta + \theta_{1/2}) > 90^\circ \end{cases} \tag{4}$$

$$\left(\beta - \theta_{1/2}\right) \le \tan^{-1}\left(\tan\theta_z \cos\gamma_s\right) \le \left(\beta + \theta_{1/2}\right) \tag{5}$$

F is a control function. It has a value of 1 if the beam radiation is incident on the CPC and zero if it is not. β is the slope angle the axis of the CPC makes with the zenith.

C. Thermal Analysis of CPC Collectors

1) Loss Coefficient

The thermal losses associated with a STPP collector system are due to convection and radiation from the receiver to ambient, and conduction, which is often neglected, from the receiver to the supporting structure. The cylindrical receiver is assumed to be evacuated with a glass cover to suppress the aforementioned losses, which can be lumped into a loss coefficient.

The loss coefficient can be calculated from the following relationship if Q_{loss}, the receiver area $A_{receiver}$ and the ΔT is known [8]:

$$\begin{aligned} \frac{Q_{loss}}{A_{receiver}} &= h_w \left(T_r - T_a\right) + \varepsilon\sigma T_r^4 - T_{sky}^4 + U_{cond}\left(T_r - T_a\right) \\ &= \left(h_w + h_r + U_{cond}\right)\left(T_r - T_a\right) \\ &= U_L \left(T_r - T_a\right) \\ \therefore \quad U_L &= \frac{Q_{loss}}{A_{receiver}\left(T_r - T_a\right)} \end{aligned} \tag{6}$$

where T refers to temperature and the subscripts r and a indicate receiver and ambient, respectively. Thus, for obtaining U_L , all the other factors in (6) must be known. Duffie [8] presents a method for obtaining Q_{loss} by iteration. He states that for a collector of certain length, the heat transfer from the receiver (at T_r) to the inside of the cover (at T_{ci}) through the cover (at T_{co}) and then to the surroundings (at T_a and T_{sky}) is given by the following relationships:

$$Q_{loss} = \frac{2\pi k_{eff} L}{\ln\left(\dfrac{D_{ci}}{D_r}\right)}\left(T_r - T_{ci}\right) + \frac{\pi D_r L \sigma\left(T_r^4 - T_{ci}^4\right)}{\dfrac{1}{\varepsilon_r} + \dfrac{1-\varepsilon_c}{\varepsilon_c}\left(\dfrac{D_r}{D_{ci}}\right)} \tag{7}$$

$$Q_{loss} = \frac{2\pi k_c L}{\ln\left(\dfrac{D_{co}}{D_{ci}}\right)}\left(T_{ci} - T_{co}\right) \tag{8}$$

$$Q_{loss} = \pi D_{co} L h_w \left(T_{co} - T_a\right) + \varepsilon_c \pi D_{co} L \sigma\left(T_{co}^4 - T_{sky}^4\right) \tag{9}$$

D refers to diameter, L to length, T to temperature and ε to emissivity. The subscripts r, ci, co, and a, represent the receiver, inner cover, outside cover and ambient, respectively. If the annulus is evacuated so that convection is suppressed, k_{eff} can be zero. The procedure for solving the preceding equations by iteration is carried out by estimating T_{co} then, calculating Q_{loss} from (9) and substituting this value in (8) to find an estimate of T_{ci} .Then (7) checks the guess of T_{co}, by comparing the calculated Q_{loss} from (9) and (7). The outside convective coefficient h_w is calculated by simultaneously solving the following equations [8]:

$$Nu = 0.3\,\mathrm{Re}^{0.6} = \frac{h_w D_{co}}{k} \tag{10}$$

where k is the thermal conductivity, and Re is the Reynolds number calculated from:

$$\mathrm{Re} = \frac{\rho V D}{\mu} \tag{11}$$

ρ is the density of the medium, V is the wind velocity and μ is the dynamic viscosity.

2) Fluid Heat Transfer Coefficient

Although fluid properties do change with variations in temperature, it is always advisable to work with average fluid heat transfer coefficient values depending on the temperature range expected in the system. The following equations help determine the fluid heat transfer coefficient, assuming turbulent flow conditions for a Reynolds' number >2200 [16].

$$h_{fi} = \frac{N_u k}{d} \tag{12}$$

where, d is the pipe diameter, N_u is the Nusselt Number and can be calculated from the following correlation:

$$N_u = 0.025 R_e^{0.79} P_r^{0.42} p \tag{13}$$

Assuming p=1.023, P_r is the Prandtl Number obtained from:

$$P_r = \frac{\mu C_p}{k} \tag{14}$$

where, μ , C_p and k are the fluid's viscosity, its specific heat and its conductivity, respectively.

3) Collector's Useful Gain

The useful gain can be seen as the rate of useful energy extracted by the collector. It is proportional to the useful energy absorbed by the collector minus the amount lost by the collector to its surroundings. It in turn depends on the overall heat transfer coefficient and the collectors' efficiency and flow factors. The overall heat transfer coefficient, U_o, can be calculated provided that the receiver's thermal conductivity (k_r) and inner (D_i) and outer (D_o) diameters are known, along with the heat transfer coefficient inside the tube (h_{fi}).

$$U_o = \left[U_L^{-1} + \frac{D_o}{h_{fi} D_i} + \left(\frac{D_o}{2k_r} \ln\left(\frac{D_o}{D_i} \right) \right) \right]^{-1} \quad (15)$$

The collector's efficiency factor and flow factor can be determined from (16) and (17), respectively:

$$F' = \frac{U_o}{U_L} = \frac{U_L^{-1}}{U_L^{-1} + \frac{D_o}{h_{fi} D_i} + \left(\frac{D_o}{2k_r} \ln\left(\frac{D_o}{D_i} \right) \right)} \quad (16)$$

$$F'' = \frac{F_R}{F'} = \frac{mC_p CR}{A_{receiver} U_L F'} \left[1 - \exp\left(- \frac{A_{receiver} U_L F'}{mC_p CR} \right) \right] \quad (17)$$

where m is the mass flow rate and C_p is the specific heat of the fluid.

The collector's useful gain is then:

$$Q_u = F_R A_{aper} \left[S - \frac{A_{receiver}}{A_{aper}} U_L \left(T_i - T_a \right) \right] \quad (18)$$

where S is the absorbed radiation per unit area of collector aperture, as discussed above. According to Duffie [8], the derivation of a collector's useful gain equation must be modified if the time period of the measured solar data is other than hours because it assumes that the time base for solar radiation data is hours, since it is the most common time period for reporting meteorological data. To account for this, the resulting energy gain equation must then be integrated over the selected time period.

After having calculated de collector's useful gain, the fluid temperature rise is found from:

$$\Delta T = \int \frac{Q_u}{mC_p} \quad (19)$$

and the exit fluid temperature is:

$$T_f = T_i + \Delta T \quad (20)$$

D. Heat Exchanger (HX) Analysis

The *heat exchanger* (HX), on the other hand, provides a means for transferring heat from the "hot" HTF to the "cold" fluid that will propel the turbine, namely water. It usually involves convection in each fluid and conduction through the wall that separates the two fluids. These effects are taken into consideration by a HX overall heat transfer coefficient, U_{HX}, which depends on the individual resistances due to convection and conduction through the pipes and wall, and on the heat exchanger geometry itself. There are usually several stages of heat exchanging process [10]. These processes can be seen in Fig. 4.

1) HX Energy Balance

The basic heat exchanger equations can be obtained by analyzing Fig. 5 and the mechanisms of heat exchange, namely, conduction and convection. Heat is transferred from the hot fluid to the inside of the wall by convection, through it by conduction, and then from the outside of the wall to the cold fluid by convection [18], [19]. The thermal resistance network can then by described by the following equation:

$$R_{total} = R_i + R_{wall} + R_o = \frac{1}{h_i A_i} + \frac{\ln\left(D_o / D_i \right)}{2\pi kL} + \frac{1}{h_o A_o} \quad (21)$$

where the subscripts *i*, *o* and *wall* refer to the inner, outer and wall resistances, respectively. It is useful to express the rate of heat transfer between the two fluids as:

$$\dot{Q} = \frac{\Delta T}{R_{total}} = U_{HX} A \Delta T = U_i A_i \Delta T = U_o A_o \Delta T \quad (22)$$

where U_{HX} is the HX overall heat transfer coefficient. The inner and outer rate of heat transfers exists because the HX has two surface areas which are not usually equal to one another. If lacking design constraints such as diameters and length, HX overall heat transfer coefficients can be found in tables [16], [18],[19]. There are two methods of HX analysis for obtaining the HX's heat transfer rate, which are: the log-mean-temperature-difference (LMTD) and the effectiveness-NTU method. They both rely on the following assumptions: HXs are steady-flow devices so kinetic and potential energy changes are negligible, the fluid's specific heat is taken as an average constant value in a specified temperature range and the HX is assumed to be perfectly insulated so there is no heat loss to the surroundings [18], [19]. Based on these assumptions and on the 1st Law of Thermodynamics, it can be said that the rate of heat transfer from the "hot" fluid be equal to the rate of heat transfer to the "cold" one:

$$\dot{Q} = \dot{m}_c C_{pc} (T_{c,out} - T_{c,in}) = \dot{m}_h C_{ph} (T_{h,in} - T_{h,out}) \quad (23)$$

where the subscripts *c* and *h* stand for cold and hot fluids, respectively. The heat capacity rate, $\dot{C}$, which is the product of the fluid's mass flow rate and its specific heat, represents the

rate of heat transfer needed to change the temperature of the fluid stream by 1°C as it flows through the HX.

$$\dot{C}_c = \dot{m}_c C_{pc}, \quad \dot{C}_h = \dot{m}_h C_{ph} \tag{24}$$

2) The Effectiveness-NTU Method

The *Effectiveness-NTU method* is used when outlet temperatures are not specified. This method is much more complex than the LMTD and is highly dependent on HX geometry and flow arrangement. It is based on the heat transfer effectiveness ε, defined as [19]:

$$\varepsilon = \frac{\dot{Q}}{\dot{Q}_{\max}} = \frac{\text{Actual heat transfer rate}}{\text{Maximum possible heat transfer rate}} \tag{25}$$

The actual heat transfer rate can be determined from the energy balance described above. The maximum possible heat transfer rate depends on the maximum temperature difference that can be achieved in a HX,

$$\Delta T_{\max} = T_{h,in} - T_{c,in} \tag{26}$$

therefore, the maximum heat transfer rate is:

$$\dot{Q}_{\max} = \dot{C}_{\min} \Delta T_{\max} \tag{27}$$

where $\dot{C}_{\min}$ is the smallest heat capacitance rate. Effectiveness relations involve the dimensionless number of transfer units or, NTU. It is expressed as:

$$NTU = \frac{UA_s}{C_{\min}} = \frac{UA_s}{(\dot{m}C_p)_{\min}} \tag{28}$$

Another useful dimensionless quantity is the capacity ratio:

$$c = \frac{C_{\min}}{C_{\max}} \tag{29}$$

For a shell-and-tube HX, the most commonly used in STPPs,

$$\varepsilon = \frac{2}{\left[1 + c + \sqrt{1+c^2}\,\frac{1+e^{-NTU\sqrt{1+c^2}}}{1-e^{-NTU\sqrt{1+c^2}}}\right]} \tag{30}$$

$$NTU = -\frac{1}{\sqrt{1+c^2}} \ln\left(\frac{\frac{2}{\varepsilon} - 1 - c - \sqrt{1+c^2}}{\frac{2}{\varepsilon} - 1 - c + \sqrt{1+c^2}}\right) \tag{31}$$

E. Thermodynamic Cycle

The *Rankine cycle* is the most commonly used cycle for electricity generation. The Rankine cycle has been proven to be the ideal cycle for vapor power plants [20]. Since its components (pump, boiler, turbine and condenser) are all steady-flow devices, the cycle can be analyzed through steady-flow equations per unit mass of steam.

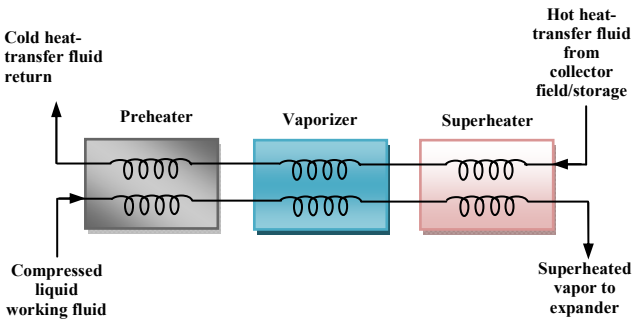

Fig. 4. Heat exchanging steps from the 'hot' to the 'cold' fluid.

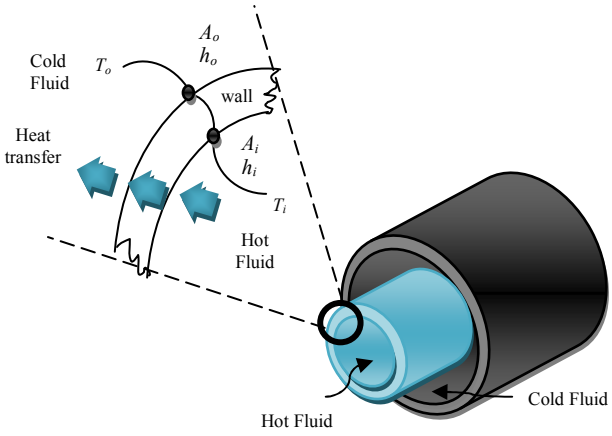

Fig. 5. Heat exchanging steps from the 'hot' to the 'cold' fluid.

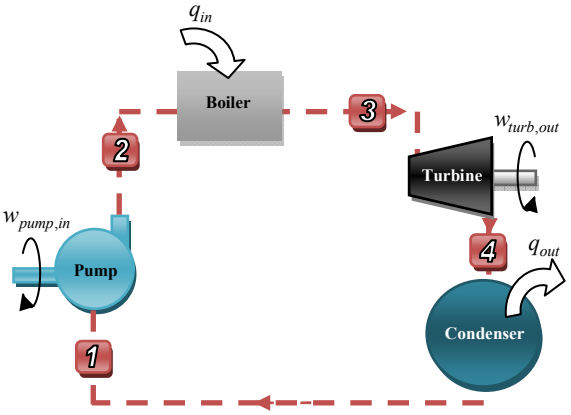

Fig. 6. Rankine cycle schematic

The boiler and condenser do not require or produce any work, and if the pump and turbine are assumed to be isentropic, then the conservation of energy relation yields [18]:

$$pump \quad w_{pump,in} = h_2 - h_1 = v\left(P_2 - P_1\right) \tag{32}$$

$$boiler \quad q_{in} = h_3 - h_2 \tag{33}$$

$$turbine \quad w_{turb,out} = h_3 - h_4 \tag{34}$$

$$condenser \quad q_{out} = h_4 - h_1 \tag{35}$$

where *w* stands for the work needed (*in*) or produced (*out*) by the *pump* or *turb*ine. *h* refers to the enthalpy in each process and, *q* represents the energy that enters (*in*) to and exits (*out*) from a process.

The thermal efficiency, η_{th}, of the Rankine cycle can be determined from the ratio of net work and the energy that enters the system, namely:

$$\eta_{th} = \frac{w_{net}}{q_{in}} = 1 - \frac{q_{out}}{q_{in}} \tag{36}$$

where,

$$w_{net} = q_{in} - q_{out} = w_{turb,out} - w_{pump,in} \tag{37}$$

IV. Case Study And Results

For the present study, an optical and thermal analysis of the CPC and absorber was conducted in Microsoft Excel® and MATLAB®. The results were used in the Simulink® model. These parameters can, however, be: estimated, taken from literature or from manufacturer's data. The HTF used in the analysis is molten salt. It is being preferred over the typical HTF, VP-1®, because it provides several advantages such as: chemical stability, can attain higher operating temperatures and can be used as the thermal energy storage (TES) medium [21]. The data used in the analysis is presented in the Appendix. Simulations for a parabolic trough solar thermal power plant can be studied in [22].

A whole year was considered for studying system performance. Only several days are presented in this paper. These are: March 20, 2002, January 28, 2003 and July 1, 2003. This is to account for a clear, cloudy and rainy day. In the following figures, atmospheric conditions regarding temperature, wind velocity and precipitation were plotted, as well as the solar radiation for each particular day. Using this data, system performance could be observed by evaluating the results obtained from the simulation model constructed. The model is capable of plotting: Solar radiation, HTF temperature exiting the collector field, the steam temperature leaving the HX and the respective power output of the system. It is important to acknowledge that several system parameters were considered constant, such as: the HTF and steam's mass flows, number of collectors per row, mass flow of HTF per row, HTF inlet temperature, condensate water temperature and pressure and the turbines' operating pressure. These parameters are carefully monitored in STPP such as: the SEGS. They provide a means of system control.

V. Conclusion

As can be seen from the plotted results in the Appendix, the fairer and clearer the day (March 20, 2002), the more solar radiation is obtained and an optimal system performance is observed. When there are solar transients due to clouds, it can be seen that the system has some drops in overall system temperature and thus, in power output. If these transients occur for brief periods of time, e.g., 5 to 10 minute intervals, the system is able to return to steady power production once solar radiation is maintained. If these solar transients are prolonged for lengthy periods, e.g., an hour or two, (January 28, 2003) then system performance is greatly reduced and the system may not recover. However, if there are solar transients due to prolonged periods of rain as can be observed on July 1, 2003, the system produces an almost zero power output once it starts to rain.

Several aspects were studied but, were not included in the simulation model for simplicity, since in most cases these could be negligible. These are: system's piping losses, collectors' optical losses and no customization of power block.

The simulation model was successfully validated by utilizing data for the SEGS VI plant presented in [22]. Even though the collector systems are not exactly the same, both system models showed a very similar thermal response.

VI. Appendix

TABLE I
DATA USED IN STPP SYSTEM MODEL

Variables	Values	
Receiver inner diameter	0.115	m
Receiver outer diameter	0.125	m
Thickness of receiver	0.005	m
Operating temperature	350	°C
Emittance of receiver	0.31	
Emittance of collector	0.88	
Thermal conductivity glass	1.4	
Glass cover outer diameter	0.148	m
Glass thickness	4	mm
Glass cover inner diameter	0.14	m
Length	1	m
Wind speed	3	m/s
Sky temperature	2	°C
Air temperature	10	°C
Conductivity of steel	16	W/m °C
Collector width	1.524	m
Collector length	12	m
Required Power Output	10	MW
Turbine Operating Temp	400	°C
Turbine Operating Pressure	4000	kPa
Turbine mass flow	14	kg/s
Condenser Temperature	106	°C
Fluid temp entering absorber	140	°C
Mass flow per collector	2	kg/s
Specific Heat (water)	4.18	kJ/kg °C
Specific Heat (salt)	1.56	kJ/kg °C
Wind convection coeff	300	W/m^2 °C

Simulation results for March 20, 2002 (clear day):

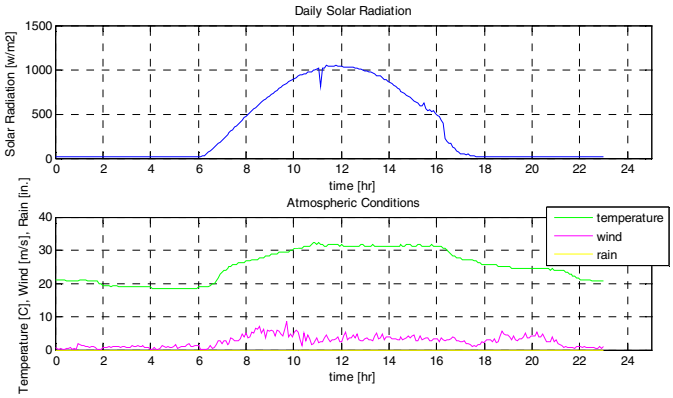

Fig. 7. Measured Solar Radiation, Ambient Temperature, Wind Velocity and Precipitation for March 20, 2002

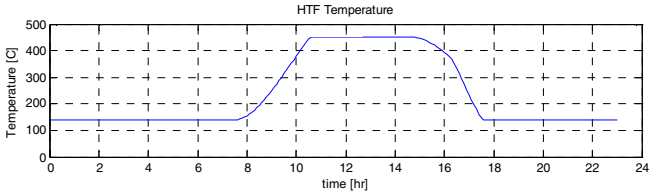

Fig. 8. HTF Temperature at the collector field outlet on March 20, 2002

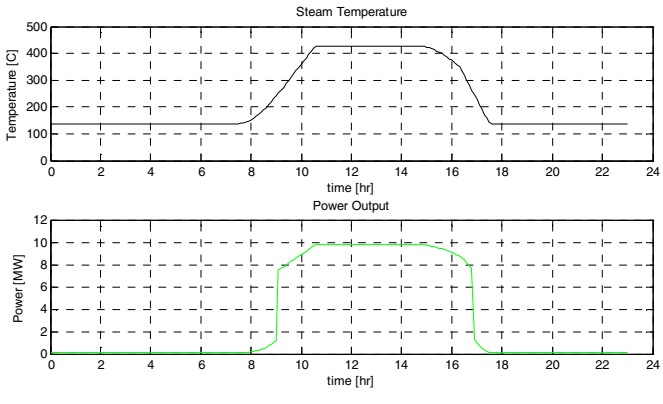

Fig. 9. Heat Exchanger Steam Temperature and the respective Power Output for March 20, 2002

Simulation results for January 28, 2003 (cloudy day):

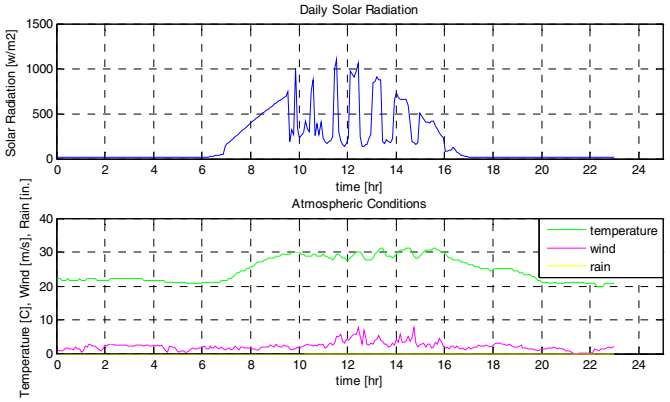

Fig. 10. Measured Solar Radiation, Ambient Temperature, Wind Velocity and Precipitation for January 28, 2003

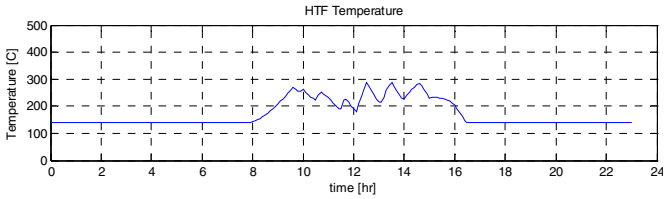

Fig. 11. HTF Temperature at the collector field outlet on January 28, 2003

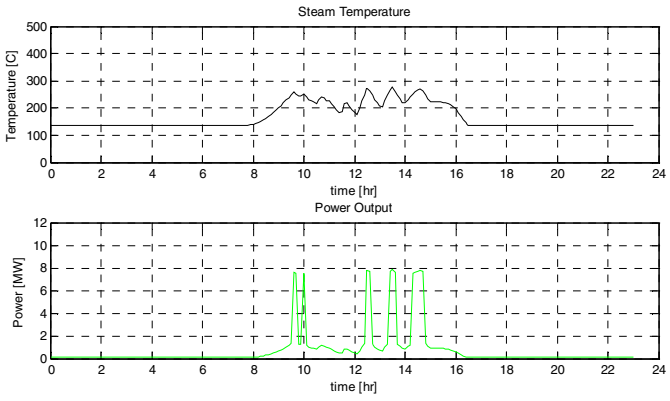

Fig. 12. Heat Exchanger Steam Temperature and the respective Power Output for January 28, 2003

Simulation results for July 1, 2003:

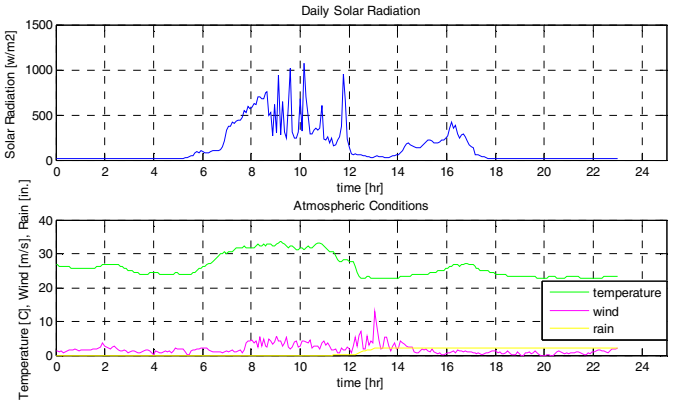

Fig. 13. Measured Solar Radiation, Ambient Temperature, Wind Velocity and Precipitation for July 1, 2003

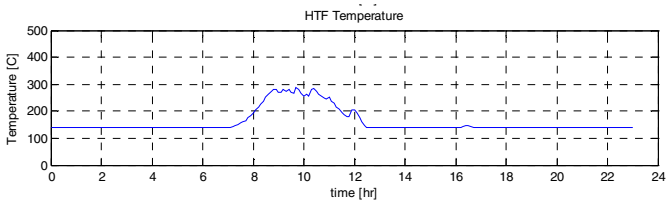

Fig. 14. HTF Temperature at the collector field outlet on July 1, 2003

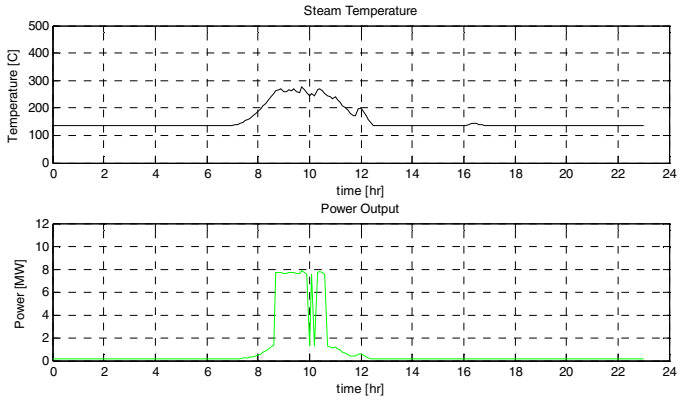

Fig. 15. Heat Exchanger Steam Temperature and the respective Power Output for July 1, 2003

VII. ACKNOWLEDGMENT

The authors gratefully acknowledge the contributions of Dr. Fernando Plá and Dr. Gustavo Gutiérrez from the Mechanical Engineering Department at UPRM. Also the authors recognize the contributions of all the members that belong to NSF Center of Power Electronics (CPES), and the Mathematical Modeling and Control of Renewable Energies for Advance Technology & Education (M_{inds}^2CREATE) Research Team at UPRM.

VIII. REFERENCES

[1] Eck, M. & Hirsch, T. Dynamics and control of parabolic trough collector loops with direct steam generation, Solar Energy, Vol. 81, pp. 268–279, 2007.

[2] Hou, H.J., Wang, Z.F, Wang, R.Z. & Wang, P.M., A new method for the measurement of solar collector time constant, Renewable Energy, Vol. 30, pp. 855–865, 2005.

[3] Jones, S.A., Pitz-Paal, R., Schwarzboezl, P., Blair, N. & Cable, R., TRNSYS Modeling of the SEGS VI Parabolic Trough Solar Electric Generating System, Proceedings of Solar Forum 200, Solar Energy: The Power to Choose April 21-25, Washington, DC, 2001.

[4] Kim, Y. & Seo, T., Thermal performances comparisons of the glass evacuated tube solar collectors with shapes of absorber tube, Renewable Energy, Vol. 32, pp. 772-795, 2007.

[5] Leutz, R.; Annen, H.P.,Energy Performance Modelling of Stationary and Quasi-Stationary Solar Concentrators Based on Reverse Ray-Tracing Photovoltaic Energy Conversion, Conf. Record of the 2006 IEEE 4th World Conf. on Photovoltaic Energy Conv., Vol. 1, pp. 714 – 717, 2006.

[6] Valera, P.; Esteban, A.; de los Reyes Carrillo, M.; Osuna, R.; Menna, P.; Gambi, R.; Helm, P.; Grottke, M.; Geyer, M.; Dobon, F.; Monedero, J.; Lugo, A.; Romero, M.; Chenlo, F.; Alonso, M.; Sanchez, M.; Artigas, J.; Fresneda, A., Solar Energy: Comparative Analysis of Solar Technologies for Electricity Production, Proceedings of 3rd World Conference on Photovoltaic Energy Conversion, 2003, Vol. 3, pp. 2482-2485, 2003.

[7] Rabl, A., Optical and Thermal Properties of Compound Parabolic Concentrators, Solar Energy, Vol. 18, pp. 497-511, 1976.

[8] Duffie, J. & Beckman, W. Solar Engineering of Thermal Processes, John Wiley & Sons, 2006.

[9] Kearney, D., Kelly, B., Herrmann, U., Cable, R., Pacheco, J., Mahoney, R., Price, H., Blake, D., Nava, P., & Potrovitza, N., Engineering Aspects of a Molten Salt Heat Transfer Fluid in a Trough Solar Field, Energy, Vol. 29, pp. 861–870, 2004.

[10] Stine, W.B. & Harrigan, R.W., Solar Energy Systems Design, John Wiley & Sons, 1985.

[11] Kennedy, C.,Terwilliger, K. & Warrick, A., Optical Durability of Candidate Solar Reflector Materials, Journal of Solar Energy Engineering, Vol. 127, pp. 262-269, 2004.

[12] Kim, Y. & Seo, T., Thermal performances comparisons of the glass evacuated tube solar collectors with shapes of absorber tube, Renewable Energy, Vol. 32, pp. 772-795, 2007.

[13] Rabl, A., Optical and Thermal Properties of Compound Parabolic Concentrators, Solar Energy, Vol. 18, pp. 497-511, 1976.

[14] Rabl, A., Practical Design Considerations for CPC Solar Collectors, Solar Energy, Vol. 22, pp. 373-381, 1979.

[15] Rabl, A., Solar Concentrators with Maximal Concentration for Cylindrical Absorbers, Applied Optics, Vol. 15, pp. 1871-1873, 1976.

[16] Incropera, F. & DeWitt, D.; Intr. to Heat Transfer, Wiley & Sons, 2002.

[17] Garg, H.P., Advances in Solar Energy Technology: Volume 1: Collection and Storage Systems, Springer, 1987.

[18] Çengel, Y.A., Introduction to Thermodynamics and Heat Transfer, McGraw-Hill, 1997.

[19] Çengel, Y.A., Turner, R.H. & Cimbala, J.M., Fundamentals of Thermal Fluid Sciences, Mc Graw-Hill, 2008.

[20] Drbal, L.F., Power Plant Engineering - Black&Veatch, Kluwer Academic Publishers, 2001.

[21] Kearney, D., Kelly, B., Herrmann, U., Cable, R., Mahoney, R., Price, H., Nava, P., Potrovitza, N., Overview on use of a Molten Salt HTF in a Trough Solar Field, NREL Parabolic Trough Thermal Energy Storage Workshop, 2003

[22] Patnode, A.M., "Simulation and Performance Evaluation of Parabolic Trough Solar Power Plants". Master's Thesis, Department of Mechanical Engineering, University of Wisconsin-Madison, 2006.

[23] Mingzhi Zhao; Zhizhang Liu; Qingzhu Zhang; "Feasibility Analysis of Constructing Parabolic Trough Solar Thermal Power Plant in Inner Mongolia of China" Asia-Pacific Power and Energy Engineering Conference, 2009. APPEEC 2009. 27-31 March 2009 Page(s):1 – 4

[24] Cabello, J.M.; Cejudo, J.M.; Luque, M.; Ruiz, F.; Deb, K.; Tewari, R.; "Optimization of the sizing of a solar thermal electricity plant: Mathematical programming versus genetic algorithms" IEEE Congress on Evolutionary Computation, 2009. 18-21 May 2009 pp:1193 – 1200

[25] Lu Jianfeng; Ding Jing; "Optimal Operating Temperature for Solar Thermal Power System" Asia-Pacific Power and Energy Engineering Conference, 2009. APPEEC 2009. 27-31 March 2009 Page(s):1 – 4

[26] Hongli Zhang; Zhifeng Wang; Minghuan Guo; Wenfeng Liang; "Cosine Efficiency Distribution of Heliostats Field of Solar Thermal Power Tower Plants" Asia-Pacific Power and Energy Engineering Conference, 2009. APPEEC 2009. 27-31 March 2009 Page(s):1 - 4